Energy Storage Sizing in Presence of Uncertainty

Sina Taheri and Vassilis Kekatos
Bradley Dept. of ECE, Virginia Tech
Blacksburg, VA 24060
Emails: {st92,kekatos}@vt.edu

Sriharsha Veeramachaneni
Windlogics Inc.,
St Paul, MN 55107
Email: Sriharsha.Veeramachaneni@windlogics.com

***Abstract*—Uncertainty is an inevitable side-effect of the increasing penetration of intermittent energy sources like solar and wind into the power grid. Since energy storage systems (ESS) can be employed to mitigate the effect of uncertainties, their energy and power ratings along with their charging control strategies become of vital importance for renewable energy producers. This work deals with the task of sizing under a model predictive control (MPC) operation for a single ESS used to smoothen out a random energy signal. To account for correlations in the energy signal and enable charging adjustments in response to real-time fluctuations, we adopt a linear charging policy. The policy is designed by minimizing the initial ESS investment plus the average operational cost. Since charging decisions become random, the energy and power limits are posed as chance constraints. Relying on first- and second-order moments for the energy signal, the chance constraints are enforced in a distributionally robust fashion. To better approximate the joint probability of acquiring feasible charging schedules, the double-sided ESS limits are handled jointly as second-order cone constraints. The proposed scheme is contrasted to a charging policy under Gaussian uncertainties and a deterministic formulation.**

***Index Terms*—Affine control policies; double-sided chance constraints; distributionally robust programs; second-order cone programs.**

I. Introduction

The uncertainty associated with renewable generation challenges optimal power system planning and dispatching. From the wind or solar energy producer's viewpoint, committing to a contract solely based on historical data and forecasts may not be optimal: The violation of such contract due to uncertainty may result in unsought and possibly extreme financial penalties. To cater for this problem, ESS can be utilized to alleviate contract deviations. Employing ESS for such purpose calls for optimal sizing and operation strategies, which are hard to solve due to two main reasons: As an investment problem, the entire lifetime of the ESS should be considered resulting in a horizon that is significantly longer than the ESS dispatch timescale. Moreover, possible uncertainties should be considered, rendering an infinite-horizon stochastic problem.

For a producer that rents ESS on a daily basis, the dynamic sizing of such ESS has been studied in [1], where wind forecasts are drawn from a normal probability distribution function (pdf). When daily ESS renting is not a viable option, a greedy heuristic for optimal ESS sizing and placement has been put forth under a linearized power flow model and perfect forecasts [2]. Considering a power system where conventional generators and energy storage are jointly dispatched, the sizing task has been tackled under Gaussian forecast errors in [3].

This work was supported by a grant from Windlogics Inc.

Chance-constrained optimization has been used for tackling different power system tasks. Assuming Gaussian uncertainty and for the purpose of optimal power flow (OPF), chance constraints have been proposed in [4], [5]. Conservative convex approximations of chance constraints for the AC OPF task has been studied in [6]. Non-Gaussian uncertainty has been tackled in [7] by estimating the cumulative distribution function (CDF) of correlated non-Gaussian random variables.

Model predictive control (MPC) schemes surrogate infinite- or long-horizon problems that are often computationally intractable, by a sequence of finite- or shorter-horizon problems. In an MPC setup, after solving the first finite-horizon problem, only the first optimal decision is implemented and the horizon is shifted forward by one time step and the process is repeated. Under a deterministic setup, the performance degradation of finite-horizon MPCs has been quantified in [8]. Although such quantifications do not exist for stochastic MPCs, the approach is known to work well in practice and it has been used for dispatching storage systems [9]. A two-stage stochastic MPC has been recently developed in [10] for ESS sizing under Gaussian wind uncertainties. Using a linearized power flow and battery degradation models, an ESS sizing approach presuming no uncertainties has been proposed in [11]. Most existing approaches either ignore uncertainty [2], [11]; or resort to sampling [1], [12].

Energy storage sizing is formulated here through a distributionally robust (DR) MPC framework. By exploiting the convex reformulation of double-sided chance constraints [6], [13], it is ensured that the worst-case probability of violating double-sided ESS limits is small for a broad family of distributions. Given the first- and second-order moments of the underlying pdf's, the ESS sizing task can be reformulated as a second-order conic program (SOCP). As a base case, a deterministic MPC formulation is also proposed, which avoids chance constraints by placing all uncertainties in the cost. The ESS sizing task is also formulated under Gaussian uncertainty and the three methods are contrasted.

II. Energy Storage Modeling and Operation

The energy storage system (ESS) is operated at control periods of fixed duration of say 15 minutes. The MPC horizon starting at control period h is indexed by h. Each MPC horizon consists of T control periods with a relative index (offset) of

$t = 0, \dots, T-1$, e.g., the t-th period within horizon h is control period $h+t$.

The charging amount during period t is denoted by b_t^h, which is positive when the battery is charging. Assuming a charging cycle of unit efficiency, the state of charge (SoC) at the end of period t within horizon h is $s_t^h = b_t^h + s_{t-1}^h$ for $t = 0, \dots T-1$. If we collect the charging amounts and the SoCs during horizon h respectively in vectors $\mathbf{b}^h := [b_0^h \cdots b_{T-1}^h]^\top$ and $\mathbf{s}^h := [s_0^h \cdots s_{T-1}^h]^\top$, the ESS dynamics can be compactly expressed as

$$\mathbf{s}^h = \mathbf{F}\mathbf{b}^h + \mathbf{1}s_{-1}^h, \quad \forall h \tag{1}$$

where $\mathbf{F}$ is a lower triangular matrix having ones in all its non-zero entries; $\mathbf{1}$ is a T-length vector of all ones; and s_{-1}^h is the SoC at the beginning of horizon h with $s_{-1}^1 = 0$.

If $\bar{p}$ and $\bar{s}$ are the power and energy ratings for the ESSs, the charging and SoC vectors are constrained as

$$-\mathbf{1}\bar{p} \leq \mathbf{b}^h \leq \mathbf{1}\bar{p} \tag{2a}$$

$$\mathbf{0} \leq \mathbf{s}^h \leq \mathbf{1}\bar{s}. \tag{2b}$$

for all h with the inequalities applied entrywise.

Based on the MPC rationale, at every horizon h, the operator solves an ESS dispatch problem for the next T control periods to find $\mathbf{b}^h$. But rather than implementing the entire $\mathbf{b}^h$, only the first charging decision b_0^h is actually taken to bring the SoC from s_{-1}^h to s_0^h. The process is repeated by initiating the MPC scheme for horizon $h+1$ with $s_{-1}^{h+1} = s_0^h$. The coupling across horizons can be captured by rewriting (1) as

$$\mathbf{s}^h = \mathbf{F}\mathbf{b}^h + \mathbf{1}\mathbf{e}_1^\top \mathbf{s}^{h-1}, \quad \forall h \tag{3}$$

where $\mathbf{e}_t$ is the t-th canonical vector of length T.

The purpose of the ESS is to smoothen out an *energy signal* p_t^h, which could be the output of a wind farm; an aggregation of solar panels; the negative of a load aggregation; the net commitment to a generation contract; or combinations thereof. The cost of deviating from this energy signal over horizon h is captured through a given function f as

$$f_h(\mathbf{b}^h) := \sum_{t=0}^{T-1} f(p_t^h - b_t^h). \tag{4}$$

The key point though is that the energy signal p_t^h is not known *a priori*. Rather, before running the MPC scheme for horizon h, we are given a forecast $(\boldsymbol{\mu}^h, \boldsymbol{\Sigma}^h)$ for the energy signal $\mathbf{p}^h := [p_0^h \cdots p_{T-1}^h]^\top$ to be experienced over the next T periods, so that

$$\mathbf{p}^h = \boldsymbol{\mu}^h + \boldsymbol{\delta}^h \tag{5}$$

where $\boldsymbol{\mu}^h := \mathbb{E}[\mathbf{p}^h]$ and $\boldsymbol{\delta}^h$ is a zero-mean random vector with covariance $\boldsymbol{\Sigma}^h$. Given that $\boldsymbol{\delta}^h$ is random, the cost in (4) becomes random, and the ESS operator is interested in minimizing the expected cost $\bar{f}_h(\mathbf{b}^h) := \mathbb{E}[f_h(\mathbf{b}^h)]$.

Having described the operational cost per MPC horizon, let us now formulate the objective of the ESS sizing problem. The ultimate goal is to decide the ESS power and energy capacities $(\bar{p}, \bar{s})$, so that the overall (operational and investment) cost is minimized. The operational cost is found as the average over H MPC horizons. If (π_p, π_s) are the amortized prices for battery sizing, our objective is to minimize

$$g(\mathbf{x}) := \frac{1}{HT}\mathbb{E}\left[\sum_{h=1}^{H}\sum_{t=0}^{T-1} f(p_t^h - b_t^h)\right] + \pi_p\bar{p} + \pi_e\bar{s} \tag{6}$$

over the charging decisions $\mathbf{b} := \{\mathbf{b}^h\}_{h=1}^H$ and the sizing variables, all collectively denoted by $\mathbf{x} := \{\mathbf{b}, \bar{p}, \bar{s}\}$.

If the contract deviation cost is of the form $f(x) = ax^2 + cx$, the average operational cost for horizon h can be shown to be

$$\bar{f}_h(\mathbf{b}^h) = a\,\mathrm{Tr}(\boldsymbol{\Sigma}^h) + a\left\|\boldsymbol{\mu}^h - \mathbf{b}^h\right\|_2^2 + c\mathbf{1}^\top(\boldsymbol{\mu}^h - \mathbf{b}^h). \tag{7}$$

The coefficients (a, c) are kept constant assuming that the contract remains invariant across time. Alternatively, if the operational cost changes over time as $f_h(x) = a_h x^2 + c_h x$ and the prices (a_h, c_h) are random but independent of $\boldsymbol{\mu}^h$, then (7) holds for $a = \mathbb{E}[a_h]$ and $c = \mathbb{E}[c_h]$.

III. Energy Storage Sizing

A. Deterministic Charging Decisions

If the charging decisions $\mathbf{b}$ are treated as deterministic, ESS sizing can be posed as minimizing (6) subject to (2)–(3)

$$\min_{\mathbf{b},\bar{p},\bar{s}} \; \frac{1}{HT}\sum_{h=1}^{H} \bar{f}_h(\mathbf{b}^h) + \pi_p\bar{p} + \pi_e\bar{s} \tag{8a}$$

$$\text{s.to} \quad -\bar{p}\mathbf{1} \leq \mathbf{b}^h \leq \bar{p}\mathbf{1}, \qquad h = 1, \dots, H \tag{8b}$$

$$\mathbf{0} \leq \mathbf{F}\mathbf{b}^h \leq \bar{s}\mathbf{1}, \qquad h = 1 \tag{8c}$$

$$\mathbf{0} \leq \mathbf{F}\mathbf{b}^h + \sum_{i=1}^{h-1} \mathbf{b}_1^i \leq \bar{s}\mathbf{1}, \qquad h = 2, \dots, H \tag{8d}$$

which can be solved as a linearly-constraint quadratic program.

As evident from (7), problem (8) ignores the intra-horizon correlations of $\boldsymbol{\delta}^h$, and thus it not yield a sufficiently large energy storage system. To cater for this shortcoming, a new charging policy is adopted next.

B. Charging Policies

To take into account the correlation across $\boldsymbol{\delta}$, one can postulate a control policy where $\mathbf{b}^h$ depends linearly on the random energy signal $\mathbf{p}^h$ as

$$\mathbf{b}^h = \mathrm{dg}(\boldsymbol{\alpha}^h)\mathbf{p}^h = \mathrm{dg}(\boldsymbol{\alpha}^h)(\boldsymbol{\mu}^h + \boldsymbol{\delta}^h) \tag{9}$$

where $\boldsymbol{\alpha}^h := [\alpha_0^h \cdots \alpha_{T-1}^h]^\top$, and $\mathrm{dg}(\boldsymbol{\alpha}^h)$ is a diagonal matrix having vector $\boldsymbol{\alpha}^h$ on its main diagonal. Rather than optimizing over deterministic $\mathbf{b}^h$ as in (8), the charging policy of (9) finds the optimal $\{\boldsymbol{\alpha}^h\}$. In this way, charging decisions adapt to the energy signal even when the latter varies within a control period. Such real-time adjustments could allow for longer control periods, i.e., smaller values of T, within each MPC horizon, thus reducing the computational burden for both the sizing and operational tasks. Similar control policies have been adopted for designing the droop parameters of synchronous generators in response to wind uncertainty at the power system level [4], [13]. Reference [10] assumes that $\boldsymbol{\alpha}^h = \mathbf{1}$, thus resulting to large ESS ratings.

To optimally design $\boldsymbol{\alpha}$ along with sizing, let us collect all $\{\boldsymbol{\alpha}^h\}$ in the HT-length vector $\boldsymbol{\alpha}$. Plugging the charging policy of (9) into (1) yields

$$\mathbf{s}^h = \mathbf{F}\,\mathrm{dg}(\boldsymbol{\alpha}^h)(\boldsymbol{\mu}^h + \boldsymbol{\delta}^h) + \mathbf{1}\sum_{i=1}^{h-1} \alpha_1^i(\mu_1^i + \delta_1^i)$$

so the t-th entry of $\mathbf{s}^h$ depends on previous forecasts as

$$s_t^h = \mathbf{e}_t^\top \mathbf{s}^h = \mathbf{e}_t^\top \mathbf{F}\,\mathrm{dg}(\boldsymbol{\alpha}^h)(\boldsymbol{\mu}^h+\boldsymbol{\delta}^h)+\sum_{i=1}^{h-1}\alpha_1^i(\mu_1^i+\delta_1^i). \quad (10)$$

Since $\boldsymbol{\delta}^h$ is random, $\mathbf{b}^h$ and $\mathbf{s}^h$ are random as well and the constraints in (2) cannot be enforced deterministically. One may want to select $\mathbf{x}$ so that (8b)–(8d) are satisfied with a prescribed probability of $1-\epsilon$. Nonetheless, guaranteeing all $4HT$ constraints are satisfied with a given probability is computationally intractable. Therefore, one may consider enforcing the instantaneous charging and SoC constraints for all h and t as [4], [3], [10]

$$\Pr(b_t^h \leq \bar{p}) \geq 1-\epsilon' \quad \text{and} \quad \Pr(-b_t^h \leq \bar{p}) \geq 1-\epsilon' \quad (11a)$$
$$\Pr(s_t^h \leq \bar{s}) \geq 1-\epsilon' \quad \text{and} \quad \Pr(-s_t^h \leq 0) \geq 1-\epsilon'. \quad (11b)$$

A better approximation of the original overall chance probability is to enforce the two single-sided constraints of (11a) into one chance constraint, and the two single-sided constraints of (11b) into another one as

$$\Pr(-\bar{p} \leq b_t^h \leq \bar{p}) \geq 1-\epsilon \quad (12a)$$
$$\Pr(0 \leq s_t^h \leq \bar{s}) \geq 1-\epsilon. \quad (12b)$$

If the violation probability in (11) is set so that $\epsilon' = \epsilon$, then (11) is a relaxation of (12). If $\epsilon' = \frac{\epsilon}{2}$, it is a restriction of (12); see [13].

To enforce the single- or double-sided constraints in (11) or (12), we next explain how the first- and second-order statistics of b_t^h and s_t^h can be expressed as affine functions of the statistics of $\{\boldsymbol{\delta}^h\}$. First collect all $\{\boldsymbol{\delta}^h\}_{h=1}^H$ in the HT-length vector $\boldsymbol{\delta}$, whose mean is zero and its covariance is $\boldsymbol{\Sigma}$. Matrix $\boldsymbol{\Sigma}$ which can be block-diagonal if forecasts are uncorrelated across MPC horizons. Block diagonal or not, the diagonal blocks of $\boldsymbol{\Sigma}$ are denoted by $\boldsymbol{\Sigma}^h$ for $h=1,\ldots,H$. Moreover, the diagonal entries of $\boldsymbol{\Sigma}^h$ is stored in vector $\boldsymbol{\sigma}^h$. From (9), the charging amount b_t^h has mean $\alpha_t^h\mu_t^h$ and variance $\left(\alpha_t^h\right)^2\sigma_t^h$. Similarly, for s_t^h we get from (10)

$$\mu(s_t^h) = \mathbf{e}_t^\top \mathbf{F}\,\mathrm{dg}(\boldsymbol{\alpha}^h)\boldsymbol{\mu}^h + \sum_{i=1}^{h-1}\alpha_1^i\mu_1^i = \boldsymbol{\alpha}^\top \mathbf{a}_t^h \quad (13)$$
$$\sigma(s_t^h) = \|\boldsymbol{\Sigma}^{1/2}\mathbf{S}_t^h\boldsymbol{\alpha}\|_2^2 \quad (14)$$

where $\boldsymbol{\Sigma}^{1/2}$ is the matrix square root of $\boldsymbol{\Sigma}$; while vector $\mathbf{a}_t^h$ and the $HT \times HT$ selection matrix $\mathbf{S}_t^h$ can be obtained from (10).

Under the charging policy of (9), the expected operational cost can be found to be

$$\tilde{f}_h(\boldsymbol{\alpha}^h) := \mathbb{E}[f_h(\boldsymbol{\alpha}^h)]$$
$$= a\cdot(\boldsymbol{\alpha}^h)^\top\left[\mathrm{dg}^2(\boldsymbol{\mu}^h)+\mathrm{dg}(\boldsymbol{\sigma}^h)\right]\boldsymbol{\alpha}^h$$
$$+\left[c\boldsymbol{\mu}^h - 2a\boldsymbol{\mu}^h\odot\boldsymbol{\mu}^h\right]^\top\boldsymbol{\alpha}^h$$
$$+a\|\boldsymbol{\mu}^h\|_2^2 + a\,\mathrm{Tr}(\boldsymbol{\Sigma}^h)+c\mathbf{1}^\top\boldsymbol{\mu}^h. \quad (15)$$

If $\boldsymbol{\delta}$ is Gaussian in particular, the constraints in (11a) can be reformulated as linear inequality constraints using the related inverse CDF [10]. Having the mean and standard deviation of b_t^h, these linear constraints for time t of horizon h become

$$-\bar{p} + \alpha_t^h(\mu_t^h + \beta_1\sigma_t^h) \leq 0 \quad (16a)$$
$$-\bar{p} - \alpha_t^h(\mu_t^h - \beta_2\sigma_t^h) \leq 0 \quad (16b)$$

where $\beta_1 := \Phi^{-1}(1-\epsilon')$; $\beta_2 := \Phi^{-1}(\epsilon')$; and Φ is the CDF of a standard normal random variable. The constraints in (11b) can be expressed as second-order cone (SOC) constraints [10]. From the mean and standard deviation of s_t^h from (13) and (14), these SOC constraints become for all t and h

$$\beta_1\|\boldsymbol{\Sigma}^{1/2}\mathbf{S}_t^h\boldsymbol{\alpha}\|_2 \leq \bar{s} - \boldsymbol{\alpha}^\top\mathbf{a}_t^h \quad (17a)$$
$$\beta_1\|\boldsymbol{\Sigma}^{1/2}\mathbf{S}_t^h\boldsymbol{\alpha}\|_2 \leq \boldsymbol{\alpha}^\top\mathbf{a}_t^h. \quad (17b)$$

The number of SOC constraints can be reduced by half by introducing an auxiliary variable c_t^h at the expense of adding two linear constraints [4]

$$c_t^h \leq \bar{s} - \boldsymbol{\alpha}^\top\mathbf{a}_t^h \quad (18a)$$
$$c_t^h \leq \boldsymbol{\alpha}^\top\mathbf{a}_t^h \quad (18b)$$
$$\beta_1\|\boldsymbol{\Sigma}^{1/2}\mathbf{S}_t^h\boldsymbol{\alpha}\|_2 \leq c_t^h. \quad (18c)$$

Therefore, the task of ESS sizing under the policy of (9) for Gaussian uncertainty $\boldsymbol{\delta}$ can be expressed as

$$\min_{\boldsymbol{\alpha},\bar{p},\bar{s}} \ \frac{1}{HT}\sum_{h=1}^H \tilde{f}_h(\boldsymbol{\alpha}^h) + \pi_p\bar{p} + \pi_e\bar{s} \quad (19)$$
$$\text{s.to} \ \ (16),(18) \quad \forall t,h$$

which can be reformulated to a SOC program (SOCP).

If the pdf of $\boldsymbol{\delta}$ is unknown, one could follow a *distributionally robust* (DR) approach. Based on the latter, the unknown pdf belongs to a family of pdfs and the constraints in (11) are guaranteed for all members of that family. This implies that each constraint is satisfied with probability larger than $1-\epsilon'$ for the worst-case pdf, where the worst case is interpreted on a per-constraint basis.

A common DR setup is to consider the family of pdf's with fixed first- and second-order moments. Given the aforesaid moments, the pdf of $\boldsymbol{\delta}$ is allowed to lie within the family $\mathcal{P}$ of zero-mean HT-length random vectors with covariance $\boldsymbol{\Sigma}$. Then, the first constraint in (11a) can be expressed as

$$\inf_{\Pr\in\mathcal{P}} \Pr(b_t^h \leq \bar{p}) \geq 1-\epsilon'$$

and can be reformulated as an SOC; see [13]. However, handling each constraint in (11) separately is suboptimal. Leveraging the results of [13], we consider the worst-case pdf for the double-sided constraints of (12). Interestingly, these constraints can still be expressed as SOCPs as reviewed next.

Consider the general feasible set incurred by a double-sided chance constraint

$$\mathcal{Z} := \left\{ \mathbf{x} : \inf_{\boldsymbol{\delta} \sim \Pr \in \mathcal{P}} \Pr\left(|\boldsymbol{\delta}^\top \mathbf{w}(\mathbf{x}) + u(\mathbf{x})| \leq v \right) \geq 1 - \epsilon \right\}$$

where the vector $\mathbf{w}(\mathbf{x})$ and the scalar $u(\mathbf{x})$ are affine functions of the optimization variable $\mathbf{x}$, while $v > 0$ is a given scalar. The constraints in (12a) and (12b) can both be expressed in form of the feasible set $\mathcal{Z}$. As established in [13], the double-sided chance constraint captured by set $\mathcal{Z}$ can be written as

$$\mathcal{Z} = \{ \mathbf{x} : y^2 + \mathbf{w}^\top(\mathbf{x}) \boldsymbol{\Sigma} \mathbf{w}(\mathbf{x}) \leq \epsilon (v - z)^2, \\ |u(\mathbf{x})| \leq y + z, \quad 0 \leq z \leq v, \quad y \geq 0 \} \tag{20}$$

where y and z are auxiliary optimization variables. Observe that the first constraint in (20) can be written as an SOC. Hence, the set $\mathcal{Z}$ in (20) has been expressed as the intersection of one SOC and five linear inequality constraints.

Applying this reformulation to ESS sizing, the pairs of doubly-sided constraints in (12) are expressed as

$$|\alpha_t^h \mu_t^h| \leq y_t^h + z_t^h \tag{21a}$$
$$0 \leq z_t^h \leq \bar{p} \tag{21b}$$
$$y_t^h \geq 0 \tag{21c}$$
$$\left\| \begin{bmatrix} \sigma_t^h \alpha_t^h \\ y_t^h \end{bmatrix} \right\|_2 \leq \sqrt{\epsilon} \left(\bar{p} - z_t^h \right) \tag{21d}$$
$$\left| \bar{s}/2 - [\mathbf{a}_t^h]^\top \boldsymbol{\alpha} \right| \leq \hat{y}_t^h + \hat{z}_t^h \tag{21e}$$
$$0 \leq \hat{z}_t^h \leq \bar{s}/2 \tag{21f}$$
$$\hat{y}_t^h \geq 0 \tag{21g}$$
$$\left\| \begin{bmatrix} \boldsymbol{\Sigma}^{1/2} \mathbf{S}_t^h \boldsymbol{\alpha} \\ \hat{y}_t^h \end{bmatrix} \right\|_2 \leq \sqrt{\epsilon} \left(\bar{s}/2 - \hat{z}_t^h \right) \tag{21h}$$

where y_t^h, z_t^h, $\hat{y}_t^h$, and $\hat{z}_t^h$ are slack variables. Constraints (21a)–(21d) correspond to (12a), and (21e)–(21h) correspond to (12b). The DR formulation has twice as many SOC constraints as its Gaussian counterpart in (19). The DR MPC can be compactly formulated as

$$\min_{\boldsymbol{\alpha}, \bar{p}, \bar{s}} \quad \frac{1}{HT} \sum_{h=1}^{H} \tilde{f}_h(\boldsymbol{\alpha}^h) + \pi_p \bar{p} + \pi_e \bar{s} \tag{22}$$
$$\text{s.to} \quad (21) \quad \forall t, h.$$

This formulation caters for the worst-case double-sided chance constraints and therefore is a more conservative than (19).

IV. Numerical Tests

The three ESS sizing methods of (8), (19), and (22) were compared through numerical tests. The mean value for the random energy signal $\mathbf{p}$ was selected to be the actual wind generation of [14]. The covariance matrix of $\boldsymbol{\delta}$ was simulated as block-diagonal with $\boldsymbol{\Sigma}^h = \mathbf{SCS}$, where $\mathbf{S}$ is a diagonal matrix with linearly increasing diagonal entries to model the increasing uncertainty as time moves forward, and the entries of $\mathbf{C}$ were taken to be $[\mathbf{C}]_{ij} := 0.9^{|i-j|}$. The amortized prices π_p and π_e were chosen to be $400/L$ (\$/10min) and $600/L$ (\$/10min) based on the lithium-ion technology taken

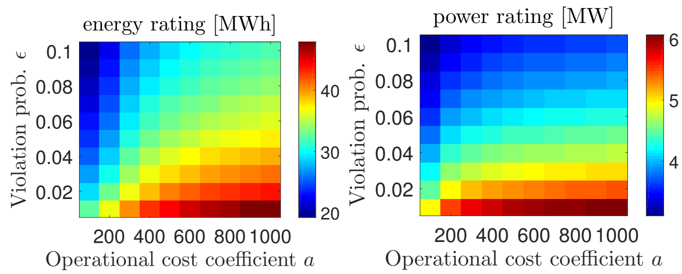

Fig. 1. Energy (left) and power (right) ratings obtained by the Gaussian formulation of (19).

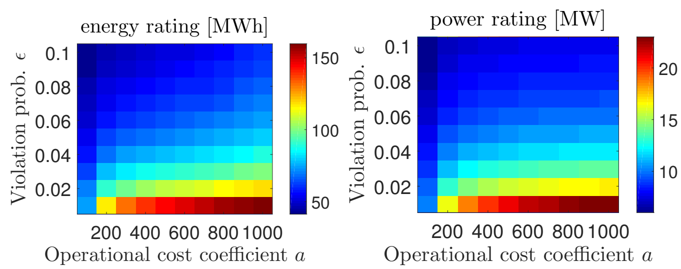

Fig. 2. Energy (left) and power (right) ratings obtained by the distributionally robust formulation of (22).

from [15], and L is the number of 10-minute time slots in the lifespan of the battery. The battery lifetime was taken to be 10 years. All tests were conducted for $H = 144$ and $T = 6$ corresponding corresponding to one day of operation of 1-hr horizons. The coefficient a in $f_h(\mathbf{b}^h)$ is termed as the penalization rate and c is set to be zero.

Figures 1 and 2 show the effect of a and the violation probability ϵ respectively for the Gaussian and DR formulations. By increasing a, having an ESS and utilizing it more is deemed more favorable than being penalized. By increasing ϵ, the constraints need to be satisfied with lower probability, meaning that smaller ESS ratings suffice.

Figure 3 depicts a comparison between the three formulations for varying a's. The DR distribution yields ESS ratings significantly larger that the other two methods, which is expected since (22) satisfies the worst-case distribution. Figure 4 depicts the effect of having a longer MPC horizons in the DR formulation. With longer horizons, the uncertainty close to the end of the horizon grows larger, and thus larger ESS will be needed to make up for it. One solution to the latter problem would be to increase the violation probability along the time periods $t = 1, \ldots, T$ within each MPC horizon. To this end, ϵ was selected as a linear function of t, and the results are contrasted to the fixed ϵ are shown in Figure 5.

V. Conclusions

Assuming an MPC control strategy, we have considered three ESS sizing formulations: a deterministic approach; a charging policy under Gaussian uncertainty; and a distributionally robust charging policy. The three formulations have been contrasted through numerical tests, which demonstrate that the DR formulation yields a higher ESS size since it

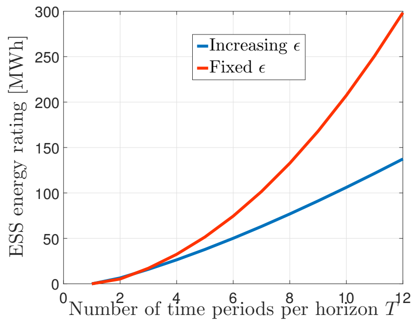

Fig. 5. Optimal ratings for increasing violation probability ϵ over t.

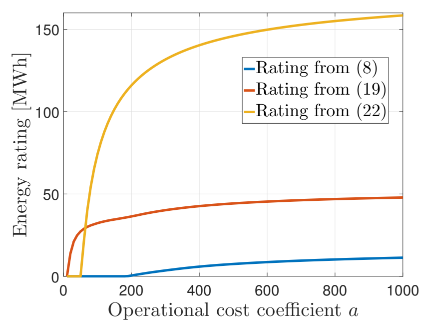

Fig. 3. Optimal energy rating for increasing operational cost a.

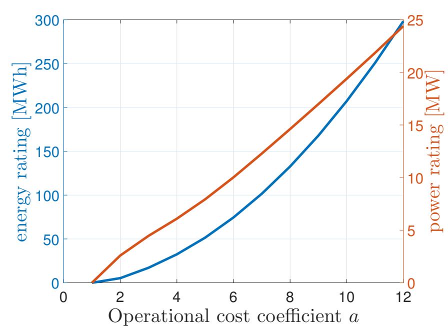

Fig. 4. Optimal ratings for increasing number of periods T per MPC horizon.

considers the worst-case pdf. The tests further demonstrate that by increasing the horizon length, the ESS size grows exponentially. To counterbalance this effect, we tried relaxing the constraint violation probability. The number of second-order cone constraints increases for increasing H, thus rendering the computational complexity prohibitive. Introducing terminal costs for MPC, numerical surrogates of chance constraints, and possible relaxations of the coupling present in ESS operation are left for future research.

References

[1] P. Pinson, G. Papaefthymiou, B. Klockl, and J. Verboomen, "Dynamic sizing of energy storage for hedging wind power forecast uncertainty," in *Proc. IEEE PES General Meeting*, Calgary, AB, Canada, Jul. 2009.

[2] K. Dvijotham, M. Chertkov, and S. Backhaus, "Storage sizing and placement through operational and uncertainty-aware simulations," in *Proc. Hawaii International Conference on System Sciences*, Waikoloa, HI, USA, Jan. 2014.

[3] A. Kargarian, G. Hug, and J. Mohammadi, "A multi-time scale co-optimization method for sizing of energy storage and fast-ramping generation," *IEEE Trans. Sustain. Energy*, vol. 7, no. 4, pp. 1351–1361, Oct. 2016.

[4] D. Bienstock, M. Chertkov, and S. Harnett, "Chance constrained optimal power flow: Risk-aware network control under uncertainty," *SIAM Review*, vol. 56, pp. 461–495, 2014.

[5] L. Roald and G. Andersson, "Chance-constrained AC optimal power flow: Reformulations and efficient algorithms," *IEEE Trans. Power Syst.*, vol. 33, no. 3, pp. 2906–2918, May 2018.

[6] E. DallAnese, K. Baker, and T. Summers, "Chance-constrained AC optimal power flow for distribution systems with renewables," *IEEE Trans. Power Syst.*, vol. 32, no. 5, pp. 3427–3438, Sep. 2017.

[7] Z. Wang, C. Shen, F. Liu, X. Wu, C. Liu, and F. Gao, "Chance-constrained economic dispatch with non-Gaussian correlated wind power uncertainty," *IEEE Trans. Power Syst.*, vol. 32, no. 6, pp. 4880–4893, Nov. 2017.

[8] L. Grune and A. Rantzer, "On the infinite horizon performance of receding horizon controllers," *IEEE Trans. Automat. Contr.*, vol. 53, no. 9, pp. 2100–2111, Oct. 2008.

[9] A. D. Giorgio, F. Liberati, A. Lanna, A. Pietrabissa, and F. D. Priscoli, "Model predictive control of energy storage systems for power tracking and shaving in distribution grids," vol. 8, no. 2, pp. 496–504, Apr. 2017.

[10] K. Baker, G. Hug, and X. Li, "Energy storage sizing taking into account forecast uncertainties and receding horizon operation," *IEEE Trans. Sustain. Energy*, vol. 8, no. 1, pp. 331–340, Jan. 2017.

[11] P. Fortenbacher, A. Ulbig, and G. Andersson, "Optimal placement and sizing of distributed battery storage in low voltage grids using receding horizon control strategies," *IEEE Trans. Power Syst.*, vol. 33, no. 3, pp. 2383–2394, May 2018.

[12] S. Dutta and R. Sharma, "Optimal storage sizing for integrating wind and load forecast uncertainties," in *Proc. IEEE Conf. on Innovative Smart Grid Technologies*, Washington, DC, USA, Jan. 2012, pp. 1–7.

[13] W. Xie and S. Ahmed, "Distributionally robust chance constrained optimal power flow with renewables: A conic reformulation," *IEEE Trans. Power Syst.*, vol. 33, no. 2, pp. 1860–1867, Mar. 2018.

[14] *Historical wind farm data*, Sotavento Galicia Foundation, accessed April 2018, http://www.sotaventogalicia.com.

[15] S. Schoenung, "Energy storage systems cost update," *SAND2011-2730*, 2011.